ELSEVIER

International Journal of Bio-Medical Computing 42 (1996) 205–214

International Journal of Bio-Medical Computing

Multispectral magnetic resonance images segmentation using fuzzy Hopfield neural network

Jzau-Sheng Lin[a], Kuo-Sheng Cheng[b,*], Chi-Wu Mao[a]

[a]*Department of Electrical Engineering, National Cheng Kung University, Tainan 70101, Taiwan, ROC*
[b]*Institute of Biomedical Engineering, National Cheng Kung University, Tainan 70101, Taiwan, ROC*

Received 13 December 1995; revised 2 May 1996; accepted 2 May 1996

Abstract

This paper demonstrates a fuzzy Hopfield neural network for segmenting multispectral MR brain images. The proposed approach is a new unsupervised 2-D Hopfield neural network based upon the fuzzy clustering technique. Its implementation consists of the combination of 2-D Hopfield neural network and fuzzy c-means clustering algorithm in order to make parallel implementation for segmenting multispectral MR brain images feasible. For generating feasible results, a fuzzy c-means clustering strategy is included in the Hopfield neural network to eliminate the need for finding weighting factors in the energy function which is formulated and based on a basic concept commonly used in pattern classification, called the 'within-class scatter matrix' principle. The suggested fuzzy c-means clustering strategy has also been proven to be convergent and to allow the network to learn more effectively than the conventional Hopfield neural network. The experimental results show that a near optimal solution can be obtained using the fuzzy Hopfield neural network based on the within-class scatter matrix.

Keywords: Multispectral images segmentation; Fuzzy Hopfield neural network; Fuzzy c-means method

1. Introduction

Segmentation (tissue classification) of the medical images obtained from magnetic resonance (MR) images is a primary step in the observation of internal anatomical soft tissues in the human body. In clinical diagnosis, MRI systems have become a standard tool for detecting a variety of tumors, lesions, and abnormalities. Differing from other diagnostic techniques, the MRI systems can produce several images, each of which emphasizes a different fundamental parameter of internal anatomical structures in the same body section with multiple contrasts, based on local variations of spin-spin relaxation time (T_2), spin-lattice relaxation time (T_1), and proton density (PD). This

* Corresponding author. Tel.: + 886 6 2757575, ext. 63424; fax: + 886 6 2343270; e-mail: kscheng@dec1.bme.ncku.edu.tw

PII S0020-7101(96)01199-3

multi-parametric nature of MRI provides the potential for greatly improved sensitivity and specificity in the detection of pathological conditions. In a sense, the images obtained from MRI systems resemble the multispectral images of the earth (LANDSAT images) obtained from remote sensing satellites.

Manual segmentation is more difficult, time-consuming, and costly than automated processing by the computer system. Due to the low tissue contrast, unclear tissue boundaries, and poor hand-eye consistency, errors sometimes occur. The advantage of generating consistent results would be offered by the automated procedures in MR images segmentation. The automated segmentation of MR images into anatomical tissues, fluids, and structures is an interesting area in MRI. In clinical medicine, tissue classification of normal and pathological tissue structures using multispectral MR images provides a great potential [1]. Several studies on the automatic recognition of normal tissues in the brain and its surrounding tissues have been proposed. In general, a quantitative strategy for the analysis of brain morphometry requires the image be segmented into different anatomic tissue components as a main step for the determination of volume, shape, and localization [2].

Multispectral classification has been described as generating better discrimination than single spectral classification [3]. Classical methods range from simple thresholding to more sophisticated techniques including methods based on local features such as the median, the variance, or the gradient. These techniques, however, do not take advantage of the multi-dimensional nature of the data [4]. It has been indicated that multispectral analysis of MR images is a valuable tool to recognize the most common normal tissues in the brain and surrounding structure [5]. The segmentation of classification of tissues obtained from multi-dimensional MRIs has been successfully employed in the past [1–10]. The analysis of such multi-dimensional images can be completed by using supervised or unsupervised classification methods. In supervised classification approaches, the region of interest (ROI) is defined by the associated human interaction and the algorithm trains on the ROI and then each pixel is flagged in the associated scenes with a given signature. The unsupervised classification approaches classify the multi-dimensional data sets without the aid of training set, but a postprocessing step is required to correct proper pixels categorized in wrong clusters.

Artificial neural networks (ANN), which have the potential in parallel processing using the hardware implementation either in a synchronous or asynchronous manner, are powerful computing systems whose architecture is made of a massive number of densely interconnected and nonlinear computing elements (called neurons). In the field of pattern recognition and decision making, ANNs have been established as a promising implementation of statistical, nonparametric, discriminant analysis because they can learn and synthesize the available information without requiring any statistical modeling of the problem [11]. The ANN systems possess some unique processing capabilities which are not found in the conventional, sequential computing systems. The architectures of ANN systems incorporating fuzzy clustering strategy have been proposed in the past [12,13]. Bezdek et al. [12] has proposed a fuzzy Kohonen clustering network which integrated the fuzzy c-means model into the learning rate and updating strategies of the Kohonen network. A feedforward, back error propagation neural network implementation of the fuzzy c-means algorithm has been derived by Davis et al. [13]. An unsupervised scheme called fuzzy Hopfield neural network (FHNN), for the classification of multi-dimensional MR images based on the within-class scatter matrix, is proposed to generate associated fuzzy partition of MR brain images in this paper.

The remainder of this paper is organized as follows. Section 2 describes the data acquisition, Section 3 reviews the fuzzy clustering techniques, Section 4 proposes the medical image segmentation using a FHNN, Section 5 shows the convergence of the FHNN on the mathematical derivations, Section 6 presents several experimental results; and finally, Section 7 gives the discussion and conclusions.

2. Data acquisition

Two separate multispectral MR images of the brain, acquired from a patient with normal physiology (Fig. 1) and one example of a patient diagnosed with a cerebral infarction in the brain (Fig. 2), are to be studied in this paper. Each multispectral image consists of five channel images formed as 256×256 pixels and 8-bit gray levels. As the reference [3], both multispectral images were acquired with T_2-weighted sequences for channel images $CH = 1$, 2, 4, and 5 and

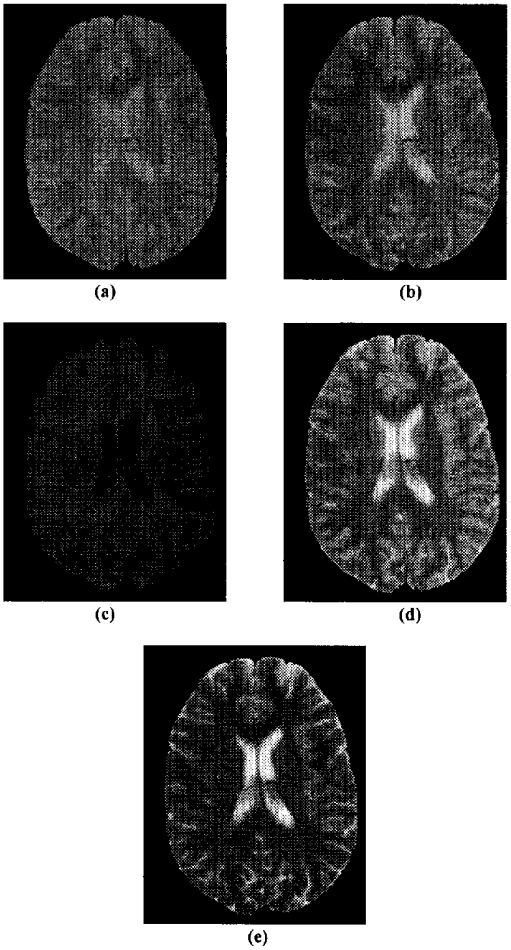

Fig. 1. The multispectral training MR brain images with normal physiology: (a) $TR_1/TE_1 = 1500$ ms/57 ms; (b) $TR_2/TE_2 = 1500$ ms/76 ms; (c) $TR_3/TE_3 = 500$ ms/20 ms; (d) $TR_4/TE_4 = 2500$ ms/75 ms; (e) $TR_5/TE_5 = 2500$ ms/100 ms.

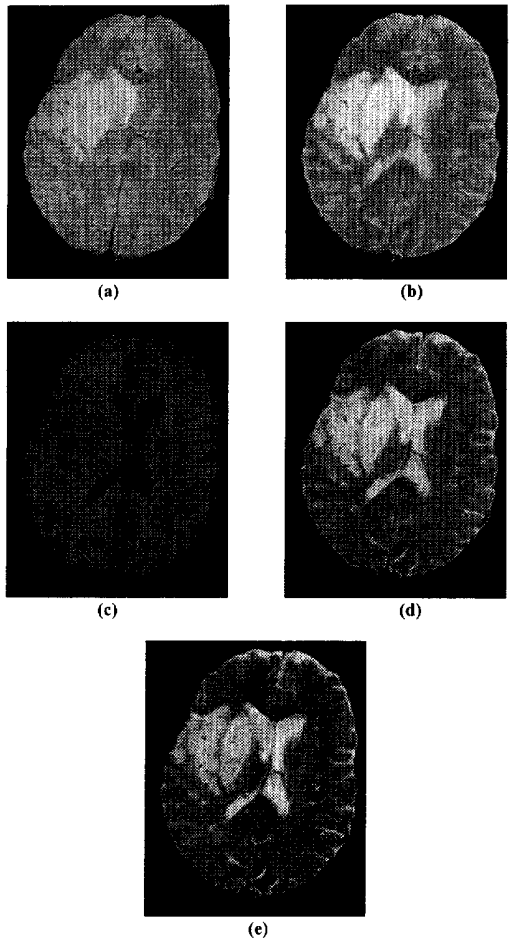

Fig. 2. The multispectral training MR images with cerebral infarction in the brain: (a) $TR_1/TE_1 = 2500$ ms/25 ms; (b) $TR_2/TE_2 = 2500$ ms/50 ms; (c) $TR_3/TE_3 = 500$ ms/20 ms; (d) $TR_4/TE_4 = 2500$ ms/75 ms; (e) $TR_5/TE_5 = 2500$ ms/100 ms.

T_1-weighted signal for channel image 3. The acquisition parameters with different repetition time (TR) and echo time (TE) are $TR_1/TE_1 = 1500$ ms/57 ms, $TR_2/TE_2 = 1500$ ms/76 ms, $TR_3/TE_3 = 500$ ms/20 ms $TR_4/TE_4 = 2500$ ms/75 ms, and $TR_5/TE_5 = 2500$ ms/100 ms for multispectral image 1 (Fig. 1) and $TR_1/TE_1 = 2500$ ms/25 ms, $TR_2/TE_2 = 2500$ ms/50 ms, $TR_3/TE_3 = 500$ ms/20 ms $TR_4/TE_4 = 2500$ ms/75 ms, and $TR_5/TE_5 = 2500$ ms/100 ms for multispectral image 2 (Fig. 2). The cerebral spinal fluid (CSF) appears bright in

the T_2-weighted image and dark in the T_1-weighted image. The T_2-weighted image shows the gray matter (GM) slightly brighter when compared with the white matter (WM), while the T_1-weighted image displays that the gray matter is darker than the white matter. The hemorrhage usually appears with cerebral infarction on a patient. The hemorrhagic infarction can be clearly depicted on the MR images. The emergent infarction area appears slightly dark, which can not be recognized easily in the T_1-weighted image. The T_2-weighted image on the other hand shows good differentiation between the infarction area and other tissues with the infarction area brighter as compared with the other tissues.

It has been pointed out that accurate measurement of white matter, gray matter, and CSF volumes in the living human brain is critical for understanding how certain diseases affect these tissues [1]. Therefore, the skin or fat and other surrounding structures in the multispectral brain images are masked into background cluster in this study. The acquisition parameters were selected to capture as much different information as possible in the five channel images. Each nonzero pixel image location then consists of five gray scale values which make up what we will refer to as a 'pixel vector.'

3. Fuzzy clustering techniques

Clustering is a process for classifying objects or patterns in such a way that samples within a cluster are more similar to one another than samples belonging to different clusters. Similarity measures employed to classify samples depend on object characteristics based on distance, vector, entropy, etc. There have been many applications based on clustering paradigms. These applications include image segmentation, speech recognition, and data comparison. Many clustering strategies have been used, such as hard clustering algorithm and soft (fuzzy) clustering algorithm, each of which has its own special characteristics. The hard clustering algorithm, for example, c-means [14,15], will converge the objective function iteratively to a local minimum from each sample to the nearest cluster centroid. However, rather than assigning each training sample to one and only one cluster, the fuzzy clustering methods assign each training sample with a degree of uncertainty described by a membership grade. A pixel's membership grade function with respect to a specific cluster indicates to what extent its properties belong to that cluster. The larger the membership grade (close to 1), the more likely that the pixel belongs to that cluster.

Fuzzy clustering strategies are mathematical tools for detecting similarities between members of a collection of samples. Since the introduction of the fuzzy set theory in 1965 by Zadeh, it has been applied in a variety of fields [1,8,10,16–19], including medical image analysis [1,8,10,16]. The theory of fuzzy logic provides a mathematical framework to capture the uncertainties associated with human cognition processes. In medical image analysis, Brandt et al. [1] proposed a fuzzy c-means approach to estimate volumes of cerebrospinal fluid (CSF), white and gray matters of the MR brain images. A fuzzy c-means clustering algorithm was applied in computerized analysis and information extraction of medical MR images by Delapaz et al. [10].

The fuzzy c-means (FCM) clustering algorithm was first introduced by Dunn [20], and the related formulation and algorithm was extended by Bezdek [21]. The FCM approach, like the conventional clustering techniques, is to minimize the criteria in the least squared error sense. For $c \geq 2$ and m any real number greater than 1, the algorithm chooses $\mu_j: X \rightarrow [0, 1]$ so that $\Sigma_j \mu_j = 1$ and $w_j \in R^d$ for $j = 1, 2, \ldots, c$ to minimize the objective function:

$$J_{FCM} = \frac{1}{2} \sum_{j=1}^{c} \sum_{i=1}^{n} (\mu_{i,j})^m \|x_i - w_j\|^2 \quad (1)$$

where $\mu_{i,j}$ is the value of the jth membership grade on the ith sample x_i. The vectors $w_1 \ldots, w_j \ldots, w_c$ can be regarded as prototypes for the clusters represented by the membership grades, and they are called cluster centroids. For the purpose of minimizing the objective function, the cluster centroids and membership grades are chosen so that a high degree of membership occurs for samples close to the corresponding

cluster centroids. The FCM algorithm, being a well-known and powerful method in clustering analysis, is reviewed as follows:

3.1. FCM algorithm

3.1.1. Step 1

Initialize the cluster centroids w_j $(2 \le j \le c)$, fuzzification parameter m $(1 \le m < \infty)$, and the value $\epsilon > 0$.

3.1.2. Step 2

Calculate the membership matrix $U = [\mu_{i,j}]$ using Eq. 2 as below.

$$\mu_{i,j} = \frac{\left(\frac{1}{(d_{i,j})^2}\right)^{1/(m-1)}}{\sum_{j=1}^{c}\left(\frac{1}{(d_{i,j})^2}\right)^{1/(m-1)}} \tag{2}$$

where $d_{i,j}$ is the Euclidean distance between training sample x_i and the class centroid w_j.

3.1.3. Step 3

Update the cluster centroids

$$w_j = \frac{1}{\sum_{i=1}^{n}(\mu_{i,j})^m}\sum_{i=1}^{n}(\mu_{i,j})^m x_i \tag{3}$$

3.1.4. Step 4

Compute $\Delta = \max(|U^{(t+1)} - U^{(t)}|)$. If $\Delta > \epsilon$ then go to Step 2; otherwise go to Step 5.

3.1.5. Step 5

Find the results for the final class centroids.

The value m, prechosen as any value from 1 to ∞, is called the fuzzification parameter (or exponential weight), and it reduces the noise sensitivity in the computation of the cluster centroids. In addition, the effect for $\mu_{i,j}$ is dependent upon the m. The larger the value m $(m > 1)$, the higher the dependence will be.

4. Fuzzy Hopfield neural network

Over the last few years, the Hopfield [22,23] neural network has been studied extensively with its features of simple architecture and potential for parallel implementation. Yang et al. [24] have analyzed both exponential and stochastic stabilities of the Hopfield neural network. Polygonal approximation using a competitive Hopfield neural network was demonstrated by Chung et al. [25]. In [25], The winner-takes-all rule has been adopted in the 2-dimensional discrete Hopfield neural network to eliminate the need for finding weighting factors in the energy function. Endocardial Boundary detection using the Hopfield neural network was described by Tsai et al. [26]; Washizawa [27] applied the Hopfield neural network to emulate saccades; optimal guidance using the Hopfield neural network was presented by Steck et al. [28]. Amatur et al. [7] used the 2-D Hopfield neural network for the segmentation of multispectral MR brain images. The Hopfield neural network is a well-known technique used for solving optimization problems based on the Lyapunov energy function. Here a conventional two-dimensional parallel Hopfield network for clustering problem is first reviewed. The network consists of $N \times c$ neurons which are fully interconnected neurons. Let $V_{x,i}$ denote the binary state of neuron (x, i) and $W_{x,i;y,j}$ be the interconnection weight between the neuron (x, i) and the neuron (y, j). A neuron (x, i) receives each neuron (y, j) with $W_{x,i;y,j}$ and a bias $I_{x,i}$ from outside can then be expressed by

$$Net_{x,i} = \sum_{y=1}^{N}\sum_{j=1}^{c} W_{x,i;y,j}V_{y,j} + I_{x,i} \tag{4}$$

and the Lyapunov energy function of the two-dimensional Hopfield network is given by

$$E = -\frac{1}{2}\sum_{x=1}^{N}\sum_{y=1}^{N}\sum_{i=1}^{c}\sum_{j=1}^{c} V_{x,i}W_{x,i;y,j}V_{y,j} - \sum_{x=1}^{N}\sum_{i=1}^{c} I_{x,i}V_{x,i} \tag{5}$$

Each column of the Hopfield neural network represents a class and each row represents a k-dimensional ($k = 5$ for this article) feature vector of a training pixel in a proper class. The network reaches a stable state when the Lyapunov energy function is minimized. For example, a neuron (x, i) in a firing state (i.e., $V_{x,i} = 1$) indicates that

pixel vector $\mathbf{z}_x$ belongs to class i. But, in the fuzzy Hopfield neural network, a neuron (x, i) in a fuzzy state indicates that pixel vector $\mathbf{z}_x$ belongs to class i with a degree of uncertainty described by a membership function.

In a multispectral image (5 channel images in this article), each pixel vector is assigned one of $n \times n$ training samples. If the number of classes c is defined in advance, then the FHNN consists of $n \times n$ by c neurons which can be conceived as a two-dimensional array. In this section, we will show that the segmentation for multispectral MR brain images can be mapped onto a 2-D Hopfield neural network so that the cost function serves as the energy function of the network. The idea is to form the energy function of the network in terms of the intra-class energy function. In the pattern recognition application, the degree of natural association is expected to be high among members belonging to the same class, and low among members of different clusters. In other words, the intraset (within-class) distance should be small. The proposed technique first assigns pixel vectors to their associated classes with an uncertain degree of membership grade in such a manner that the Euclidean distance between arbitrary samples and their cluster centroid is minimized. This is referred to as the intra-class assignment. In linear discriminate analysis [29], the concept of within-class scatter matrix is widely used for class separability. The iteratively and synchronously updated synaptic weight between the neuronal interconnections will gradually force the network to converge into a stable state where its energy function is minimized.

Using the within-class scatter matrix criteria, the optimization problem can be mapped into a two-dimensional Hopfield neural network with the fuzzy c-means strategy for the segmentation of multispectral MR brain images. The total weighted input for neuron (x, i) and Lyapunov energy in k-dimensional image, as defined in Eqs. 4 and 5, can be modified as

$$Net_{x,i} = |\mathbf{z}_x - \mathbf{w}_i|^2 + I_{x,i} = \sum_{p=1}^{k} \left[z_{x,p} - \sum_{y=1}^{n \times n} W_{(x,i;y,i),p} (\mu_{y,i})^m \right]^2 + I_{x,i} \tag{6}$$

and

$$E = \frac{1}{2} \sum_{x=1}^{n \times n} \sum_{i=1}^{c} (\mu_{x,i})^m \times \sum_{p=1}^{k} \left[z_{x,p} - \sum_{y=1}^{n \times n} W_{(x,i;y,i),p} (\mu_{y,i})^m \right]^2 - \sum_{x=1}^{n \times n} \sum_{i=1}^{c} I_{x,i} (\mu_{x,i})^m, \tag{7}$$

where $|\cdot|$ is the Euclidean distance in k-dimensional features, $\Sigma_{y=1}^{n \times n} W_{(x,i;y,i),p} (\mu_{y,i})^m$ is the total weighted input received from the component at dimension p of neuron (y, i) in row i, $\mu_{x,i}$ is the output state at neuron (x, i), and m is the fuzzification parameter. Each column of this modified Hopfield network represents a class and each row represents a pixel vector in a proper class. The network reaches a stable state when the modified Lyapunov energy function is minimized. For example, a neuron (x, i) in a maximum membership state indicates that pixel vector $\mathbf{z}_x$ belongs to class i.

Using the within-class scatter matrix criteria and in order to generate an adequate classification, we define the objective function as follows:

$$E = \frac{A}{2} \sum_{x=1}^{n \times n} \sum_{i=1}^{c} (\mu_{x,i})^m \times \sum_{p=1}^{k} \left[z_{x,p} - \sum_{y=1}^{n \times n} \frac{1}{\sum_{h=1}^{n \times n} (\mu_{h,i})^m} z_{y,p} (\mu_{y,i})^m \right]^2 + \frac{B}{2} \left[\left(\sum_{x=1}^{n \times n} \sum_{i=1}^{c} \mu_{x,i} \right) - n \times n \right]^2 \tag{8}$$

where E is the total intra-class scatter energy that accounts for the scattered energies distributed by all pixel vectors in the same class with a membership grade, and both $z_{x,p}$ and $z_{y,p}$ are the trained pixel components in dimension p at rows x and y respectively.

The first term in Eq. 8 is the within-class scatter energy which is the Euclidean distance between samples and the cluster centroid over c clusters. The second term guarantees that the $n \times n$ samples in $\mathbf{Z}$ can only be distributed among these c classes. More specifically, the second term, which is the penalty term, imposes constraints on the

objective function and the first term minimizes the intra-class Euclidean distance from a pixel vector to the cluster centroid in any given cluster.

As mentioned in reference [25], the quality of classification result is very sensitive to the weighting factors. Searching for optimal values for these weighting factors is expected to be time-consuming and laborious. To alleviate this problem, a 2-D Hopfield neural network with a fuzzy c-means clustering strategy, called FHNN, is proposed so that the penalty terms can be handled more efficiently. All the neurons on the same row compete with one another to determine which neuron is the maximum membership value belonging to class i. In other words, the summation of the membership state in the same row equals 1, and the total membership states in all n rows equal n. This also ensures that all training pixel vectors will be classified into these c classes. The modified Hopfield neural network FHNN enables the scatter energy function to converge rapidly into a minimum value. Then, the scatter energy of the FHNN can be further simplified as

$$E = \frac{1}{2} \sum_{x=1}^{n \times n} \sum_{i=1}^{c} (\mu_{x,i})^m \times \sum_{p=1}^{k} \left[z_{x,p} - \sum_{y=1}^{n \times n} \frac{1}{\sum_{h=1}^{n \times n} (\mu_{h,i})^m} z_{y,p} (\mu_{y,i})^m \right]^2 \quad (9)$$

By using Eq. 9, which is a modification of Eq. 8, the minimization of energy E is greatly simplified since it contains only one term and hence the requirement of having to determine the weighting factors A and B vanishes. Comparing Eq. 9 with the modified Lyapunov function Eq. 7, the synaptic interconnection weights and the bias input can be obtained as

$$W_{(x,i;y,j),p} = \frac{1}{\sum_{h=1}^{n \times n} (\mu_{h,i})^m} z_{y,p}, \quad (10)$$

and

$$I_{x,i} = 0. \quad (11)$$

By introducing Eqs. 10 and 11 into Eq. 6, the input to neuron (x, i) can be expressed as

$$Net_{x,i} = \sum_{p=1}^{k} \left[z_{x,p} - \sum_{y=1}^{n \times n} \frac{1}{\sum_{h=1}^{n \times n} (\mu_{h,i})^m} z_{y,p} (\mu_{y,i})^m \right]^2. \quad (12)$$

Consequently, the input-output function (i.e., membership function) for the x-th row is given as

$$\mu_{x,i} = \left[\sum_{j=1}^{c} \left(\frac{Net_{x,i}}{Net_{x,j}} \right)^{1/m-1} \right]^{-1} \quad \text{for all } i. \quad (13)$$

Using Eqs. 9, 12 and 13, the FHNN can classify c clusters in a parallel manner which is described as follows:

4.1. FHNN algorithm

4.1.1. Step 1

Input a set of training pixel vectors $\mathbf{Z} = \{z_1, z_2, \ldots, z_{n \times n}\}$, fuzzification parameter m ($1 \leq m < \infty$), the number of clusters c, and randomly initialize the states for all neurons $U = [\mu_{x,i}]$ (membership matrix).

4.1.2. Step 2

Compute the weighted matrix using Eq. 10.

4.1.3. Step 3

Calculate the input to each neuron (x, i):

$$Net_{x,i} = \sum_{p=1}^{k} \left[z_{x,p} - \sum_{y=1}^{n \times n} \frac{1}{\sum_{h=1}^{n \times n} (\mu_{h,i})^m} z_{y,p} (\mu_{y,i})^m \right]^2.$$

4.1.4. Step 4

Apply Eq. 13 to update the neuron's membership value in a synchronous manner.

4.1.5. Step 5

Compute $\Delta = \max (|U^{(t+1)} - U^{(t)}|)$. If $\Delta > \epsilon$, then go to Step 2, otherwise go to Step 6.

4.1.6. Step 6

Find the results for the final membership matrix with a defuzzification process.

In Step 3, the inputs are calculated for all neurons. In Step 4, the fuzzy c-means clustering method is applied to determine the fuzzy state with the synchronous process. Here, a syn-

chronous iteration is defined as an updated fuzzy state for all neurons using a software simulation.

In the last step, a defuzzification process used in [30] is applied to the fuzzy partition data to obtain the final segmentation. A pixel is assigned to a cluster when its membership grade in that cluster is larger than 0.5. If none of its membership grades satisfy this criteria, then the class possessing the maximum grade is chosen, provided that the sum of the largest two grades is greater than 0.5, and that these two clusters are neighboring clusters in terms of the distance measure. Therefore, no ambiguity in segmentation is encountered.

5. Convergence of the FHNN

Proof of the convergence of the FHNN is important because it guarantees that the network evolution will reach a stable state. The scatter energy function can be rewritten as follows:

$$E=\frac{1}{2}\sum_{i=1}^{c}\sum_{x=1}^{n\times n}(\mu_{x,i})^m \times\sum_{p=1}^{k}\left[z_{x,p}-\sum_{y=1}^{n\times n}\frac{1}{\sum_{h=1}^{n\times n}(\mu_{h,i})^m}z_{y,p}(\mu_{y,i})^m\right]^2 \tag{14}$$

which implies that

$$E\le\frac{1}{2}\sum_{i=1}^{c}\sum_{x=1}^{n\times n} \times\sum_{p=1}^{k}\left[z_{x,p}-\sum_{y=1}^{n\times n}\frac{1}{\sum_{h=1}^{n\times n}(\mu_{h,i})^m}z_{y,p}(\mu_{y,i})^m\right]^2. \tag{15}$$

Eq. 15 shows that the objective energy is less than or equal to the total distance between training samples and the cluster centroids. This proves that E is bounded from below.

Eq. 14, the same as Eq. 1, is based on a least-squared errors criteria, and it is rewritten as follows:

$$E=\frac{1}{2}\sum_{i=1}^{c}\sum_{x=1}^{n\times n}(\mu_{x,i})^m|z_x-w_i|^2 \tag{16}$$

and

$$w_i=\sum_{p=1}^{k}\sum_{y=1}^{n\times n}\frac{1}{\sum_{h=1}^{n\times n}(\mu_{h,i})^m}z^{y,p}(\mu_{y,i})^m\vec{a}_p, \tag{17}$$

where $\mathbf{w}_i$ (cluster centroid i) is the total interconnection weight received from all neurons x in the same column i and $\vec{a}_p$ is the unit vector in dimension p. Thus the reassignment of a membership degree belonging to cluster i in trained vector $\mathbf{z}_x$ will result in a decrease of the objective energy function whenever $\mathbf{z}_x$ is located closer to a feasible cluster centroid. Consequently, the FHNN will converge to a satisfactory result after several iterations of updating the reassignment matrix.

6. Experimental results

In order to generate near optimal segmented results using the FHNN, the network-associated parameter such as fuzzification parameter (m) is set at 1.5. To begin the segmentation, a random membership grade matrix, from which the prototypical centroid for each cluster can be calculated for each of the five channel images in the initial condition, must be provided for the proposed FHNN. If the initial centroid values are far from the final solution values, then more iterations will be required to converge to a feasible result. The final results was observed in repeated tests to be independent of the choice of initial cluster centroids. The segmented images are shown in Fig. 3a and b, respectively. Due to the spectral variability in the medical image data, setting constraints on the energy function for smoothing the noise is difficult. The segmented image may exhibit proper pixels categorized in wrong clusters. Such errors can be reduced by a majority filter [31] in postclassification filtering. Using the majority filter, a moving mask is passed over the whole segmented image. Multiple passes can be performed to control the degree of smoothness at the expense of losing some small local structures.

In Fig. 3a, the segmented result can outline the CSF, the white matter, and the gray matter from

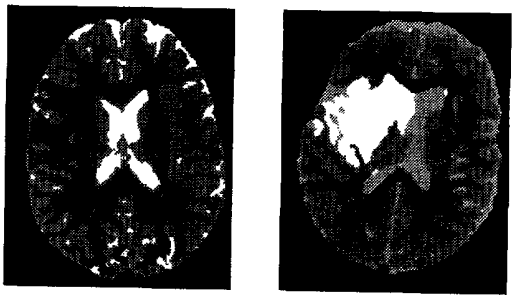

(a) (b)

Fig. 3. Classified images: (a) labeled from Fig. 1; (b) labeled from Fig. 2.

the normal transaxial MR images of the brain shown in Fig. 1. Fig. 3b is the classification map with 5 classes from Fig. 2. From the map, it can be found that the cerebral infarction region has been well delineated along with white matter, gray matter, and CSF in the lateral ventricles. To test the classification accuracy, the confusion matrices were calculated on both multispectral images. In such matrices, each element is the percentage of pixel vectors, identified as the feasible row tissues, which belong to clusters depicted in the associated column tissues. The diagonal element C_{ii} is the percentage of pixel vectors belonging to cluster i that has been correctly classified; the off-diagonal element C_{ij} is the percentage of pixel vectors belonging to cluster i that has been misclassified as belonging to cluster j. In Table 1, the correct classification rates ranging from 94.4% (CSF) to 99.7% (BKG) were achieved using the segmented solution of the multispectral training MR brain images with normal physiology, while the performance ranging from 89.5% (CI) to 99. 8% (BKG)

Table 1
Confusion matrix for the proposed FHNN using multispectral training MR brain images with normal physiology

Cluster	BKG	CSF	WM	GM
BKG	99.7	0	0.2	0.1
CSF	0	94.4	4.7	0.9
WM	3.3	0.2	95.5	1.0
GM	0	2.2	0.6	97.2

BKG, background; CSF, cerebrospinal fluid; WM, white matter; GM, gray matter.

Table 2
Confusion matrix for the proposed FHNN using multispectral training MR images with cerebral infarction to the brain

Cluster	BKG	CSF	WM	GM	CI
BKG	99.8	0	0.2	0	0
CSF	0	91.7	6.4	1.7	0.2
WM	0	0.4	93.6	5.8	0.2
GM	0	2.3	4.3	92.2	1.2
CI	0	7.1	0.5	2.9	89.5

BKG, background; CSF, cerebrospinal fluid; WM, white matter; GM, gray matter; CI, cerebral infarction.

was completed and shown in Table 2 using the classified results of multispectral training MR brain images with cerebral infarction.

7. Discussion and Conclusions

The proposed FHNN algorithm for tissues classification of multi-spectral MR images is investigated to compute automatically with no operator intervention in this study. Using the FHNN, the correct classification rates estimated in the training procedure indicate that the normal and abnormal tissues region can well be separated in the lateral ventricles. The confusion matrics give the summary statistics of the various tissues of the brain. Accurate classification of white matter, gray matter, and CSF in the brain is critical for understanding how certain diseases affect these tissues. Just regarding gray matter, white matter, CSF, and the abnormal tissue (the main tissues in the human brain), the correct classification rates were increased in the multispectral MR images segmentation.

This approach requires setting a number of different compartments in the test images, as well as a fuzzification parameter (m) that determines the amount of overlap of cluster boundaries. It can be found that within a fairly wide range of value of m, the overall result is stable, and that the final result is independent of the initial clusters centroids in the experiments. Though the fuzzy reasoning may take more computation time, the fuzzy Hopfield neural network can provide a more efficient mechanism and a greater potential

to multispectral images segmentation in parallel processing using the hardware implementation.

References

[1] Brandt ME, Bohan TP and Kramer LA: Estimation of CSF and gray matter volumes in hydrocephalic children using fuzzy clustering of MR images, *Comp Med Imaging Graph*, 18 (1994) 25–34.

[2] Kennedy DN, Filipek PA and Caviness Jr. VS: Anatomic segmentation and volumetric calculations in nuclear magnetic resonance imaging. *IEEE Trans. Med. Imaging*, 8 (1989) 1–7.

[3] Vannier M, Pilgram T, Speidel C, Neumann L, Rickman D and Schertz L: Validation of magnetic resonance imaging (MRI) multispectral tissue classification, *Comp Med Imaging Graph*, 15 (1991) 217–223.

[4] Ozkan M, Dawant BM and Maciunas RJ: Neural-network-based segmentation of multi-modal medical images: a comparative and prospective study, *IEEE Trans Med Imaging*, 12 (1993) 534–544.

[5] Taxt T and Lundervold A: Multispectral analysis of the brain using magnetic resonance imaging, *IEEE Tram Med Imaging*, 13 (1994) 470–481.

[6] Cagnoni S, Coppini G, Rucci M, Caramella D and Valli G: Neural network segmentation of magnetic resonance spin echo images of the brain, *J Biomed Eng*, 15 (1993) 355–362.

[7] Amatur SC, Piriano D and Takefuji Y: Optimization neural networks for the segmentation of magnetic resonance images, *IEEE Trans Med Imaging*, 11 (1992) 215–220.

[8] Hall LO, Bensaid AM, Clarke LP, Velthuizen RP, Silbiger MS and Bezdek JC: A comparison of neural network and fuzzy clustering techniques in segmenting magnetic resonance images of the brain, *IEEE Trans Neural Networks*, 3 (1992) 672–682.

[9] Vannier MW, Butterfield RL, Jordan D, Murphy WA, Levitt RG and Gado M: Multispectral analysis of magnetic resonance images, *Radiology*, 154 (1985) 221–224.

[10] Delapaz RL and Bernstein R: Computerized analysis and information extraction of medical magnetic resonance images (MRI), *Proc SPIE*, 902 (1988) 151–154.

[11] Tourassi GD and Floyd Jr. CE: Lesion size quantification in SPECT using an artificial neural network classification approach, *Comp Biomed Res*, 28 (1995) 257–270.

[12] Bezdek JC, Tsao ECK and Pal NR: Fuzzy Kohonen clustering networks, *Proc. IEEE Int. Conf Fuzzy Systems*, San Diego, 1992, pp. 1035–1043.

[13] Davis JP, Warms TM and Winters WR: A neural net implementation of the fuzzy c-means clustering algorithm, *Proc. IEEE Int. Joint Conf Neural Network, Seatle*, 11 (1991) A-953.

[14] Bobrowski L and Bezdek JC: C-Means clustering with l_1 and l_∞ norms, *IEEE Trans Syst Man Cybernet*, 21 (1991) 545–554.

[15] Yin PY and Chen LH: A new non-iterative approach for clustering, *Pattern Recognition Lett*, 15 (1994) 125–133.

[16] Gesu VD: Integrated fuzzy clustering, *Fuzzy Sets Syst*, 68 (1994) 293–308.

[17] Yang MS: On a class of fuzzy classification maximum likelihood procedures, *Fuzzy Sets Syst*, 57 (1993) 365–373.

[18] Yang MS and Su CF: On parameter estimation for normal mixtures based on fuzzy clustering algorithms, *Fuzzy Sets Syst*, 68 (1994) 13–28.

[19] Yoshinari Y, Pedrycz W and Hirota K: Construction of fuzzy models through clustering techniques, *Fuzzy Sets Syst*, 54 (1993) 157–165.

[20] Dunn JC: A fuzzy relative of the ISODATA process and its use in detecting compact well-separated clusters, *Cybern*, 3 (1974) 32–57.

[21] Bezdek JC: *Fuzzy Mathematics in Pattern Classification*, PhD Dissertation, Applied Mathematics, Cornell University, Ithaca, New York, 1973.

[22] Hopfield JJ and Tank DW: Neural computation of decisions in optimization problems, *Biol Cybern*, 52 (1985) 141–152.

[23] Hopfield JJ: Neural networks and physical systems with emergent collective computational abilities, *Proc Nat Acad Sci*, 79 (1982) 2554–2558.

[24] Yang H and Dillon TS: Exponential stability and oscillation of Hopfield graded response neural network, *IEEE Trans. Neural Networks*, 5 (1994) 719–729.

[25] Chung PC, Tsai CT, Chen EL and Sun YN: Polygonal approximation using a competitive Hopfield neural network, *Pattern Recognition*, 26 (1994) 1505–1512.

[26] Tsai CT, Sun YN, Chung PC and Lee JS: Endocardial Boundary detection using a neural network, *Pattern Recognition*, 26 (1993) 1057–1068.

[27] Washizawa T: Application of Hopfield network to saccades, *IEEE Trans Neural Networks*, 4 (1993) 995–997.

[28] Steck JE and Balakrishnan SN: Use of Hopfield neural networks in optimal guidance, *IEEE Trans Aerospace Electron Syst*, 30 (1994) 287–293.

[29] Fukunaga K: *Introduction to Statistical Pattern Recognition*, Academic Press, New York, 1972.

[30] Du L, Lee JS and Mango SA: Fuzzy classification of earth terrain covers using multi-look polarimetric SAR image data, *Proc IGARSS*, 4 (1993) 1602–1604.

[31] Lillesand TM and Kiefer RW: *Remote Sensing and Image Interpretation*, Wiley, New York, 1987.